Estimation of Wrist Angle from Sonomyography Using Support Vector Machine and Artificial Neural Network Models

Hong-Bo Xie [1,3], Yong-Ping Zheng [1,2 *], Jing-Yi Guo [1], Xin Chen [1], Jun Shi [1,4]

[1]Department of Health Technology and Informatics, [2]Research Institute of Innovative Products and Technologies, The Hong Kong Polytechnic University, Hong Kong, China

[3]Department of Biomedical Engineering, Jiangsu University, Zhenjiang, China

[4]School of Communication and Information Engineering, Shanghai University, China

Running Title:

Wrist Angle Estimation from SMG

[*]Corresponding Author:
Yong-Ping Zheng, PhD
Department of Health Technology and Informatics,
The Hong Kong Polytechnic University,
Hung Hom, Kowloon, Hong Kong SAR, P.R.China
Tel: 852-27667664
Fax: 852-23624365
Email: xiehb@sjtu.org (Dr. Hong-Bo Xie)
ypzheng@ieee.org (Dr. Yong-Ping Zheng)

Submitted to Medical Engineering and Physics
First submission: Jan 2 2008
First Revision: May 10 2008

Abstract

Sonomyography (SMG) is the signal we previously termed to describe muscle contraction using real-time muscle thickness changes extracted from ultrasound images. In this paper, we used least squares support vector machine (LS-SVM) and artificial neural networks (ANN) to predict dynamic wrist angles from SMG signals. Synchronized wrist angle and SMG signals from the extensor carpi radialis muscles of 5 normal subjects were recorded during the process of wrist extension and flexion at rates of 15, 22.5, 30 cycles/min, respectively. An LS-SVM model together with back-propagation (BP) and radial basis function (RBF) artificial neural networks (ANN) was developed and trained using the data sets collected at the rate of 22.5cycles/min for each subject. The established LS-SVM and ANN models were then used to predict the wrist angles for the remained data sets obtained at different extension rates. It was found that the wrist angle signals collected at different rates could be accurately predicted by all the three methods, based on the values of root mean square difference (RMSD < 0.2) and the correlation coefficient (CC > 0.98), with the performance of the LS-SVM model being significantly better (RMSD < 0.15, CC > 0.99) than those of its counterparts. The results also demonstrated that the models established for the rate of 22.5cycles/m could be used for the prediction from SMG data sets obtained under other extension rates. It was concluded that the wrist angle could be precisely estimated from the thickness changes of the extensor carpi radialis using LS-SVM or ANN models.

Keywords: Sonomyography, SMG, ultrasound, muscle, wrist angle prediction, electromyography, EMG, least squares support vector machine, SVM, artificial neural network, ANN

1. Introduction

Electromyography (EMG) is a direct reflection of muscle activity and various analyses have been carried out to investigate the relationship between the features of EMG patterns and muscle forces [1], joint angles [2], joint moments [3], and joint torques and trajectory [4, 5]. Previously, we have proposed sonomyography (SMG), which is the signal about the real-time change of muscle thickness during contraction extracted from ultrasound images of muscles, as an alternative signal to analyze muscle contraction [6-9]. The relationships between SMG and joint angle [6, 9], joint moment [10], as well as muscle fatigue [8] have been investigated. It has been demonstrated in these studies that SMG appears to have a close relationship with the change of the corresponding joint angle. However, no quantitative analysis has been conducted to understand the performance of predicting the joint angle using SMG signals.

Simple linear regression used in earlier studies [6, 9] can only provide a statistical estimation for the correlation between SMG and joint angle. The assumption of a linear input–output connection makes it not suitable for describing the complex and nonlinear relationship between SMG/EMG activities and the resultant dynamic or kinematic patterns [1, 6, 9]. Artificial neural network (ANN) is the most popular alternative method used to map the nonlinear relationship in previous studies. Sepulveda et al. [2] first made use of a three-layer feed-forward neural network model with the back-propagation algorithm in a supervised manner to map transformations between EMG and joint angle and joint moment. Similar approaches with different improvements have been adopted by researchers for studying the relationships between EMG and muscle force [1], arm movement [5], and elbow joint torque [11]. Some other ANN architectures have also been proposed for the muscle system investigation in neurophysiology and biomechanics, such as

Levenberg-Marquardt algorithm [4], time-delayed ANN [12], back-propagation (BP) through time algorithm [13].

Support vector machine (SVM), also a machine learning algorithm, was developed by Vapnik and his co-workers [14]. The SVM implements the structural risk minimization principle (SRM) rather than the empirical risk minimization principle implemented by most traditional ANN models. It seeks to minimize the upper bound of the generalization error rather than minimizing the training error [15, 16]. SVMs achieve an optimum network structure by striking a correct balance between the empirical error and the Vapnik-Chervonenkis (VC)-confidence interval which is the function of the number of training samples and the capacity of a learning machine etc [14], resulting in better generalization performance in comparison with neural network models. Although SVM was developed for pattern recognition problems [15], it has been applied to EMG related neuromuscular disease diagnosis [17, 18], sonography based decision making in the diagnosis of breast cancer [19], and many other fields [20-24]. In most of these cases, the performance of SVM modeling either matched or was significantly better than that of ANN approaches.

Despite the success in other fields, the possibility of using SVM to characterize the relationship between muscle activities and the resultant dynamical or kinematic patterns has hardly been investigated. Therefore, the aim of this paper is to examine the feasibility of applying SVM for wrist angle prediction from the SMG signal by comparing the performance of SVM and those ANN models.

2. Methods

2.1 Support vector machine

The structural diagram of least squares support vector machine (LS-SVM) applied in our present work is shown in Fig. 1. For more detailed descriptions of SVM, readers can refer to the general introductions to SVM [14, 25, 26], and tutorials on support vector classification (SVC) [15] and support vector regression (SVR) [16]. Consider a set of training samples $G = \{(x_i, y_i)\}_i^N$ (x_i is the input vector, y_i is the desired value and N is the total number of data patterns). The basic idea of support vector machine for regression is to map the data x into a high dimensional feature space via a nonlinear mapping and to perform a linear regression in this feature space:

$$y = f(x) = w^T \varphi(x) + b \quad (1)$$

where φ is a mostly nonlinear mapping function, and w and b are the weight vector and bias term, respectively. Then, minimization of the following cost function is formulated in the framework of empirical risk minimization

$$C = \frac{1}{2} w^T w + \frac{1}{2} \gamma \sum_{i=1}^{N} e_i^2 \quad (2)$$

with subject to equality constraints:

$$y_i = w^T \varphi(x_i) + b + e_i, \qquad i = 1, 2, \cdots, N \quad (3)$$

where e_i is the random errors and γ is a regularization parameter in determining the trade-off between minimizing the training errors and minimizing the model complexity.

In this nonlinear optimization problem, the Lagrangian is,

$$L = \frac{1}{2} \| w \|^2 + \gamma \sum_{i=1}^{N} e_i^2 - \sum \alpha_i \{ w^T \varphi(x_i) + b - e_i - y_i \} \quad (4)$$

where α_i are Lagrange multipliers. In order to obtain the optimum, setting partial first derivations of Eq. (7) with respect to w, b, e_i, α_i to zero,

$$\frac{\partial L(w,b,e,\alpha)}{\partial w} = 0 \rightarrow w = \sum_{i=1}^{N} \alpha_i \varphi(x_i) \tag{5}$$

$$\frac{\partial L(w,b,e,\alpha)}{\partial b} = 0 \rightarrow \sum_{i=1}^{N} \alpha_i = 0 \tag{6}$$

$$\frac{\partial L(w,b,e,\alpha)}{\partial e_i} = 0 \rightarrow \alpha_i = \gamma e_i \qquad i = 1,2,\cdots,N \tag{7}$$

$$\frac{\partial L(w,b,e,\alpha)}{\partial \alpha_i} = 0 \rightarrow w^T(\varphi(x_i) + b + e_i - y_i) = 0 \quad i = 1,2,\cdots,N \tag{8}$$

After elimination of e_i and w, the solution is given by the following set of linear equations:

$$\begin{bmatrix} 0 & \vec{1}^T \\ \vec{1} & \Omega + \gamma^{-1} I \end{bmatrix} \begin{bmatrix} b \\ a \end{bmatrix} = \begin{bmatrix} 0 \\ y \end{bmatrix} \tag{9}$$

where $y = [y_1, y_2, \cdots, y_N]$, $\vec{1} = [1,1,\cdots,1]$, $\alpha = [\alpha_1, \alpha_2, \cdots, \alpha_N]$

and the Mercer condition

$$\begin{aligned} \Omega_{kl} &= \varphi(x_k)\varphi(x_l) \\ &= K(x_k, x_l) \qquad k,l = 1,2,\cdots,N \end{aligned} \tag{10}$$

has been applied. This finally results the following LS-SVM model for function regression

$$y(x) = \sum_{i=1}^{N} \alpha_i K(x, x_i) + b \tag{11}$$

where α, b are the solutions of Eq. 9 and K kernel function.

For an input vector x_j to be tested, Eq. 11 becomes:

$$y_j = \sum_{i=1}^{N} \alpha_i K(x_j, x_i) + b \tag{12}$$

Any function that meets Mercer's condition [16] can be used as the kernel function. Currently, popular kernel functions in SVM include sigmoid kernel, polynomial kernel and Gaussian kernel, etc. In the present work, the Gaussian kernel was selected as kernel function as

$$K(x, x_i) = \exp\{-(x - x_i)^2 / 2\delta^2\} \tag{13}$$

where δ^2 is the scale factor.

To achieve a high level of performance with LS-SVM models, some parameters have to be tuned, including the regularization parameter γ and the kernel parameter corresponding to the kernel type, δ^2.

2.2 Artificial neural networks

BP neural network. BP network is a feed-forward network with an error back-propagation algorithm, one of the simplest ANN implementations. It has an input layer of source nodes, one or more layers of hidden neurons and an output layer. The back-propagation training algorithm involves two phases. During the forward phase, the neural nodes' output is specified, and the input signal is propagated through the network layer by layer. This phase finishes with the computation of an error signal between the desired response (measured muscle activation) and the actual output (predicted muscle activation) produced by the network. During the backward phase, the error signal is propagated through the network in the backward direction. It is during this phase that adjustments are applied to the free parameters of the network so as to minimize the error in a statistical sense. In spite of many applications of BP ANN [27], it suffers from a main drawback of low convergence speed [28]. Due to large amount of literatures and publications on the design, training and application of BP network introduced above and RBF network in the next section, here we just give a brief introduction of them for completeness. For detailed tutorials on their mathematical descriptions, the readers can refer to previous publications [27-29].

RBF neural network. RBF network is a member of the feed-forward neural networks, which has both unsupervised and supervised training phases [29, 30]. It was developed aiming at the defects of BP network with an improved convergence rate and better initial weights determination [28]. In the unsupervised phase, the input data are clustered and cluster details are sent to the hidden neurons, where radial basis functions of the inputs are computed by making use of the center and the standard deviation of the clusters. The learning between hidden layer and output layer is of supervised learning type where ordinary least squares technique is used. As a consequence, the weights of the connections between the kernel layer (also called hidden layer) and the output layer are determined. Thus, it comprises a hybrid of unsupervised and supervised learning.

2.3. Experiments

Five healthy subjects (three males and two females) participated in this study (age: 27.6 ± 2.9 years). None of them had history of any neuromuscular disorder and each gave written informed consent prior to the experiment.

The subject was seated in a chair with his forearm on the table, and asked to perform wrist extension starting from the neutral position and returning to the neutral position repeatedly. The subject was instructed to avoid moving the wrist into any flexion state during the test. Occasionally, some subjects might experience a very small degree of flexion, resulting in a very small negative wrist angle. It was neglected in the analysis. The term “flexion” in the following description means the action of returning from an extension state to the neutral position. After several warm-up contractions, the subject was asked to perform wrist extension and flexion guided by a metronome (MT-40, Wittner, Germany) at three extension rates of 15, 22.5, 30 cycles/min, respectively. For each extension rate, three repeated tests were performed with a rest of 3 minutes between two adjacent trials and there were three wrist extension cycles in each trial. The sonography of a cross-sectional area of the extensor carpi radialis muscle was recorded using a portable B-mode ultrasound scanner with a 7.5 MHz 38mm linear probe (180 Plus, Sonosite Inc., Washington, USA) during the continuous wrist extension and flexion. The video output of B-mode ultrasound scanner was digitized by a video capture card (PCI-1411, National Instruments, Autstin, USA) at a frame rate of 12 Hz. An electronic goniometer (XM110, Penny & Giles Biometrics, Inc. UK) was used for monitoring the wrist angle and its output signal was digitized by a data acquisition card (PCI-6024E, National Instruments, Austin, USA). The ultrasound images were saved frame by frame and synchronized with the wrist angle signal for the subsequent analysis and a total of 200 frames were saved for every trial. The diagram of the experiment setup is shown in Fig. 2 and Fig. 3 shows a typical cross-sectional ultrasound image obtained from the subject.

A cross-correlation algorithm was used to track the displacements of the interested tissue interfaces in the images using a custom-made program [9]. The details of the tracking technique can be found in reference [9]. The SMG signal, defined as the percentage change of the muscle thickness obtained at each frame could thus be recorded. The initial muscle thickness was measured at neutral position of the wrist. The typical SMG signal at three different extension rates and the SMG-wrist angle relationship are shown in Figs. 4 and 5, respectively.

2.4. Data analysis

The LS-SVM, BP and RBF ANN models of each subject were designed and implemented using Matlab software (Version 6.5, MathWorks, Inc., Massachusetts, USA). The SMG features and the actual wrist angle measured by the goniometer were employed to construct input-output pairs to train the models. The dimension of input vector was five which was formed by the current and past four SMG values. A similar feature vector constitution method was used in several previous EMG-based kinematic models [1, 33]. One set of data for each subject obtained at the extension rate of 22.5 cycles/min was selected to train the models to determine the relations between the SMG and wrist angles. The data from the remaining trials with different extension rate were used for cross-validation tests.

According to Eqs. (9), (12) and (13), it can be noted that the user has to adjust two hyperparameters, i.e., γ and δ^2 of LS-SVM. Without knowing the best values for these hyperparameters, all LS-SVM wrist angle functions could not achieve high generalization. In order to select the best values for these hyperparameters, cross validation was often applied [16] but it is rather time consuming. In this study, Bayesian inference procedure was applied to automatically find out the most appropriate values for hyperparameters γ and δ^2, which eliminated the burden of manual cross-validation procedure to estimate the values [26, 34].

The BP network used in this study had 20 nodes in hidden layer and one node in the output layer. The maximum training epoch was 10000. The learning rate was set to be 0.1 and the momentum term was 0.7. The hidden nodes used the sigmoid transfer function and the output node used the linear transfer function. The RBF network architecture used in this study was a single hidden layer with Gaussian RBF. The maximum number of hidden unit was set based on the number of the training sample and the spread parameter of RBF, which determined the smoothness of the function approximation. It was selected to be 40 in this study.

Evaluation of the wrist angle predictions from the SMG signals was made by calculating the root mean square difference (RMSD) and the correlation coefficients (CC) of the measured wrist angles and estimated values. The value of RMSD was obtained as follow:

$$RMSD = \sqrt{\frac{\sum_i (\theta(i) - \theta(i)')^2}{\sum_i (\theta(i))^2}} \tag{14}$$

where $\theta(i)$ is the measured wrist angle, and the $\theta(i)'$ is the estimated wrist angle. Predictions were considered excellent if the coefficient of cross-correlation was greater than 0.9 and the RMSD error was smaller than 15% [1]. To statistically compare the performances among the three methods, one-way analysis of variance (ANOVA) was performed [31, 32].

3. Results

The whole data set of the test at the extension rate of 22.5 cycles/min was used to determine the optimal LS-SVM tuning parameters before training the LS-SVM and the result is shown in Table 1. The training result of LS-SVM using the data obtained from subject C and the corresponding hyperparameters in Table 1 is illustrated as an example in Fig. 6. The achieved RMSD and CC of this example were 3.51% and 0.999, respectively. It was demonstrated that the wrist angles measured and predicted by LS-SVM could hardly be distinguished (Fig. 6).

The training results obtained using BP and RBF neural networks were similar to that by LS-SVM. For example, the RMSD of BP and RBF networks training for the same data from subject C was 2.84% and 4.07%, respectively. This demonstrated that the BP and RBF neural network models had a similar learning power to the LS-SVM.

The RMSD and CC between the predicted and measured angle signals were calculated for each data set of each subject. The averaged results among subjects for different extension rates are shown in Figs. 7 and 8 and examples of measured wrist angle signal and the signal predicted by the three methods for subject C at extension rates of 15, 22.5, 30 cycles/min are displayed in Figs. 9-11, respectively. It was found that prediction CC of the three models for each test condition was all larger than 0.9, with LS-SVM having the highest CC among all test conditions, followed by RBF network and BP network.. Moreover, the RMSDs of LS-SVM at the three different extension rates were all smaller than those of BP and RBF networks. The results revealed that LS-SVM had better generalization power compared with BP and RBF networks for the wrist angle prediction, though they all showed good learning power during the training. It was also demonstrated that the models established for the rate of 22.5 cycles/min could be used for the prediction of wrist angles from SMG data set obtained under other rates. Statistical analysis showed that LS-SVM achieved significantly higher prediction accuracy and CC as compared with BP, RBF networks ($p<0.05$), while no significant difference between BP and RBF methods was observed ($p>0.05$) (Tables 2 and 3).

4. Discussion and Conclusions

In our preliminary study, SMG signals had been applied to train and test the wrist angle prediction model for the data set obtained at the same extension rate of 22.5 cycles/min and within the same trial [7], i.e. using the first half of data for training and the remained for testing. In the present work, it was demonstrated that the models established for the rate of 22.5 cycles/min could be used for the prediction task of SMG data sets obtained under other rates and within different trials. Erfanian et al. [35] reported the use of EMG signals obtained from surface electrodes to determine the knee joint angle in paraplegic subjects when the quadriceps muscle was electrically stimulated using percutaneous intramuscular electrodes. They found that the peak amplitude of the evoked EMG signal and its power spectrum increased as the joint angle increased. Suryanarayanan et al. [33] developed a neural network model to estimate joint angle at the elbow using the EMG signal of biceps as an input. However, there was only one subject in their trials and the prediction

RMSD error was as large as 20%. Compared with these EMG-based modeling, the present SMG-based joint angle prediction models demonstrated better performances. Moreover, the EMG-angle relationship in the literature remained controversial and unsolved. For example, Leedham [36] and Vredenbregt et al. [37] claimed that the EMG activity was the same at different joint angles under maximum contraction of biceps brachii muscle. This is not consistent with the EMG-elbow joint angle prediction model of Suryanarayanan et al. [33]. Joint angle models reportedly heavily relied on the EMG inputs to 'drive' them. It has been demonstrated that the EMG relates more to the input of muscle contraction, i.e. the intension of an action, while the muscle architecture is a primary determination of muscle function [8]. As the architectural changes of skeletal muscle were claimed to correlate more with output of muscle contraction, and could be detected using ultrasound images [8, 9, 38]. Therefore, SMG has potential to be a better candidate to describe the relationship between joint angle patterns and the activities of corresponding muscles during the wrist extension-flexion.

The previous studies on non-parameter modeling for muscle systems were mostly based on ANN. This study investigated the feasibility of using LS-SVM method for wrist angle prediction. The experimental results in the present study indicated that the LS-SVM model performed better in comparison with the BP and RBF ANN models in terms of prediction accuracy and correlation coefficient. It was demonstrated that the LS-SVM model outperformed the BP ANN used by Suryanarayanan et al. [33] and Shi et al. [7] to predict the joint angle from the EMG and SMG signals, respectively.

In the present study, only single channel SMG signal was obtained from the extensor carpi radialis muscle and the wrist movement was limited to the extension. To improve the wrist angle prediction performance, SMG signal extracted from the flexor carpi ulnaris and other forearm muscles may be added to the model input in the future work. With multi-channel SMG data, it is believed that the predication performance be improved, as the information of different muscles contributing to the same action can be combined. Moreover, other biomedical or biomechanical signals such as mechanomyography (MMG) may be employed to provide complementary information of muscle movement behaviors. Thus, combination of SMG and MMG could potentially offer richer input features for identifying the relationship between muscle activity and arm kinematics during the execution of motor tasks. In addition, further studies are required to investigate whether the findings in this study could be applied to the movements of other joints.

In the prediction of joint angle using the SMG signal, a number of factors, including the location of ultrasound sensor, image resolution, algorithm for tracking ultrasound image, and the frame rate of ultrasound image, may affect the prediction performance. Due to the limitation of the hardware, the data rate of SMG was only 12 Hz in the present study. It is difficult to capture rapid movements of the joint. The frame rate should be improved in future studies together with improvement of image resolution and performance of the image tracking algorithm and proper procedure for the selection of measurement location. Similar to EMG, some kinds of standard protocol should be established for the data collection and analysis for SMG signals in the future studies. The real-time requirements for the LS-SVM and ANN models should also be investigated for some applications.

In summary, this study demonstrated that the wrist angle could be accurately estimated from the muscle deformation signal, i.e. SMG, using the LS-SVM and ANN models. The results also revealed that the estimation performance of LS-SVM model was significantly better than that of

ANN models. Accurate joint angle prediction is crucial for human-computer interface devices in many different areas. There have been growing interests in determining the joint angles in different areas, such as functional electrical stimulation (FES), prosthesis control, virtual reality, telerobotics and medical hand function assessment [39, 40]. Therefore, the models developed in the current study could potentially offer a feedback signal of the wrist joint extension-flexion angle for wrist position control in these areas.

Acknowledgements

This work was supported by The Hong Kong Polytechnic University (G-YE22, 1-BB69), The Hong Kong Research Grant Council (PolyU 5331/06E) and The Jiangsu University (07JDG40), PRC.

Conflict of Interest Statement

This project has not got any support from persons or companies that may cause conflict of interest.

References

[1] Liu M M, Herzog W, Savelberg H H. Dynamic muscle force predictions from EMG: an artificial neural network approach. J. Electromyogr. Kinesiol 1999; 9: 391–400.

[2] Sepulveda F, Wells D M, Vaughan C L. A neural network representation of electromyography and joint dynamics in human gait. J. Biomech 1993; 26: 101–9.

[3] Wang L, Buchanan T S. Prediction of joint moments using a neural network model of muscle activations from EMG signals. IEEE Trans Neural Sys Rehabil Eng 2002; 10: 30–7.

[4] Hahn M E. Feasibility of estimating isokinetic knee torque using a neural network model. J. Biomech 2007; 40: 1107–14.

[5] Koike Y, Kawato M. Estimation of dynamic joint torques and trajectory formation from surface electromyography signals using a neural network model. Biol Cybern 1995; 73: 1015–24.

[6] Guo J Y, Zheng Y P, Huang Q H, Chen X. Dynamic Monitoring of Forearm Muscles Using 1D Sonomyography (SMG) systems. J Rehabil Res Dev 2008; 45: 187-96.

[7] Shi J, Zheng Y P, Yan Z Z, Huang Q H. Prediction of wrist angle from sonomyography Signals with artificial neural networks technique. In: 28th Annual International Conference of the IEEE Engineering in Medicine and Biology Society. 2006. p. 3549–52.

[8] Shi J, ZhengY P, Chen X, Huang Q H. Assessment of muscle fatigue using sonomyography: Muscle thickness change detected from ultrasound images. Med Eng Phys 2007; 29: 472–9.

[9] Zheng Y P, Chan MMF, Shi J, Chen X, Huang Q H. Sonomyography: Monitoring morphological changes of forearm muscles in actions with the feasibility for the control of powered prosthesis. Med Eng Phys 2006; 28: 405–15.

[10] Shi J, ZhengY P, Chen X, Huang Q H. Relationships among continuous Sonomyography,

Electromyography and torque generated by normal upper arm muscles during isometric contraction. IEEE Trans Biomed Eng 2008; 55: 1191-8.

[11] Luh J J, Chang G C, Cheng C K, Lai J S, Kuo T S. Isokinetic elbow joint torques estimation from surface EMG and joint kinematic data: Using an artificial neural network model. J. Electromyogr Kinesiol 1999; 9: 173–83.

[12] Au A T C, Kirsch R F. EMG-based prediction of shoulder and elbow kinematics in able-bodied and spinal cord injured individuals. IEEE Trans Rehabil Eng 2000; 8: 471–80.

[13] Dipietro L, Sabatini A M, Dario P. Artificial neural network model of the mapping between electromyographic activation and trajectory patterns in free-arm movements. Med Biol Eng Comput 2003; 41: 124–32.

[14] Vapnik V. Estimation of Dependencies Based on Empirical Data. , Berlin: Springer; 1982.

[15] Burges C J C. A tutorial on support vector machines for pattern recognition. Data Min Knowl Disc 1998; 2: 121–67.

[16] Smola A J, Scholkopf B. A tutorial on support vector regression. Stat Comput 2004; 14: 199–222.

[17] Güler N F, Kocer S. Use of support vector machines and neural network in diagnosis of neuromuscular disorders. J Med Syst 2005; 29: 271–84.

[18] Xie H B, Wang Z H, Huang H, Qin C. Support vector machine in computer aided clinical Electromyography. In: Proceedings of the Second InternatIona1 Conference on Machine Learning and Cybernetics, Xi’an, 2003; p. 1106–8.

[19] Huang Y L, Chen D R. Support vector machines in sonography application to decision making in the diagnosis of breast cancer. J Clin Imaging 2005; 29: 179–84.

[20] Mohandes M A, Halawani T O, Rehman S, Hussain A A. Support vector machines for wind speed prediction. Renew Energ 2004; 29: 939–47.

[21] Shin K S, Lee1 T S, Kim H J. An application of support vector machines in bankruptcy prediction model. Expert Syst Appl 2005; 28: 127–35.

[22] Tay F E H, Cao L. Application of support vector machines in financial time series forecasting. Omega 2001; 29: 309–17.

[23] Vonga C M, Wong P K, Li Y P. Prediction of automotive engine power and torque using least squares support vector machines and Bayesian inference. Eng Appl Artif Intel 2006; 19: 277–87.

[24] Yu X, Liong S Y. Forecasting of hydrologic time series with ridge regression in feature space. J Hydrol 2007; 332: 290–302.

[25] Cristianini N, Shawe-Taylor J. An introduction to support vector machines and other kernel-based learning methods. Cambridge, UK: Cambridge Univ. Press. 2000.

[26] Suykens J A K, Gestel T V, Brabanter J D, Moor B D, Vandewalle J. Least squares support vector machines. Singapore: World Scientific Publishing. 2002.

[27] Hornik K, Stinchcommbe M, White H. Multilayer feedforward networks are universal approximators. Neural Networks 1989; 2: 359–66.

[28] Haykin S. Neural Networks, a Comprehensive Foundation. 2nd ed. Upper Saddle River, NJ: Prentice-Hall, 1999.

[29] Kasabov K. Foundations of neural network fuzzy systems and knowledge engineering. MIT. Press, 1996.

[30] Powell M J D. The theory of radial basis functions approximation, in advance of numerical analysis. Oxd Charendon Press, 1992, p.105-210.

[31] Castillo-Valdivieso P A, Merelo J J, Prieto A, Rojas I, Romero G. Statistical analysis of the parameters of a neuro-genetic algorithm. IEEE Trans. Neural Netw 2002;13: 1374–94.

[32] Wang G, Yan Z G, Hu X, Xie H B, Wang Z Z. Classification of surface EMG signals using harmonic wavelet packet transform. Physiol Meas 2006; 27: 1255–67.

[33] Suryanarayanan S, Reddy N P, Gupta V. Artificial neural networks for estimation of joint angle from EMG signals. In: IEEE 17th Annual Conference of Engineering in Medicine and Biology Society, Vol. 1, 1995, p. 823–24.

[34] Van Gestel T, Suykens J A K, Baestaens D E, Lambrechts D, Lanckriet A, Lanckriet G, Vandaele B, De Moor B, Vandewalle J. Financial time series prediction using least squares support vector machines within the evidence framework. IEEE Trans Neural Netw Special Issue on Financial Engineering 2001; 12: 809–21.

[35] Erfanian A, Chizeck H J, Hashemi R M. The relationship between joint angle and evoked EMG in electrically stimulated muscle. In: Proceedings of the 16th Annual International Conference of the IEEE Engineering in Medicine and Biology, Vol.1, 1994, p. 345–6.

[36] Leedham J S, Dowling J J. Force-length, torque-angle and EMG-joint angle relationships of the human in vivo biceps brachii. Eur J Appl Physiol 1995; 70: 421–6.

[37] Vredenbregt J, Rau G. Surface electromyography in relation to force, muscle length and endurance. In: Desmedt, J.E., editor: New developments in electromyography and clinical neurophysiology, 1. Basel: S. Karger 1973, p. 607–22.

[38] Hodges P W, Pengel L H M, Herbert R D. Measurement of muscle contraction with

ultrasound imaging. Muscle Nerve 2003; 27: 682–92.

[39] Crago P E, Memberg W D, Usey M K, Keith M W, Kirsch R F, Chapman G J, Katorgi M A, Perreault E J. An Elbow Extension Neuroprosthesis for Individuals with Tetraplegia. IEEE Trans Rehabil Eng 1998; 6: 1–6.

[40] Hart R L, Kilgore K L, Peckham P H. A Comparison between control methods for implanted FES hand-grasp systems. IEEE Trans Rehabil Eng 1998; 6 208–18.

Figure captions

Figure 1. Structural diagram of LS-SVM used in study

Figure 2. Diagram of the experimental setup

Figure 3. A typical cross-sectional ultrasound image

Figure 4. Typical SMG signals recorded at extensor carpi radialis muscle during different wrist extension rates

Figure 5. The relationship between SMG and wrist angle

Figure 6. Comparison of the predicted and measured wrist angles of wrist movement at 22.5 cycles/min by LS-SVM

Figure 7. The mean and standard deviation of prediction RMSDs across subjects at extension rates of 15, 22.5, 30 cycles/min, by LS-SVM, BP and RBF network methods

Figure 8. The mean and standard deviation of prediction CCs across subjects at 15, 22.5, 30 cycles/min extension rate by LS-SVM, BP and RBF network methods

Figure 9. Comparison of the predicted and measured wrist angles at an extension rate of 15 cycles/min by LS-SVM, BP and RBF network

Figure 10. Comparison of the predicted and measured wrist angles at an extension rate of 22.5 cycles/min by LS-SVM, BP and RBF network

Figure 11. Comparison of the predicted and measured wrist angles at an extension rate of 30 cycles/min by LS-SVM, BP and RBF network

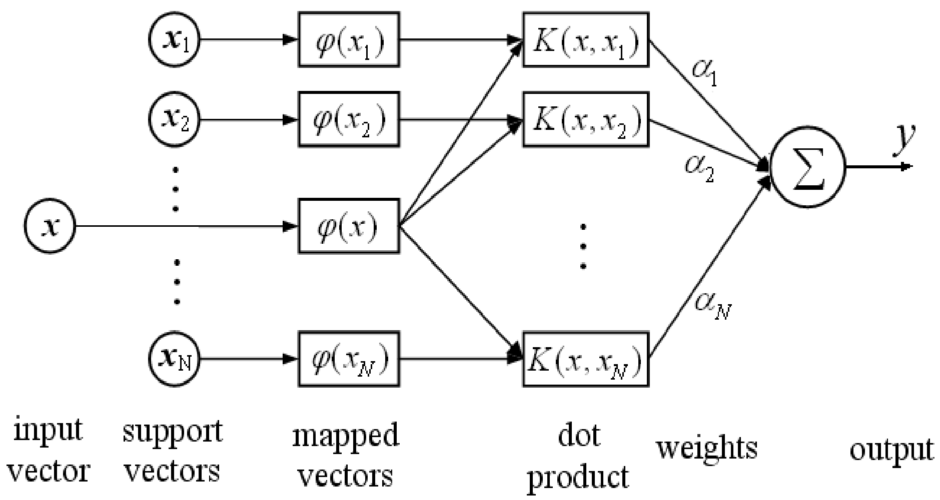

Figure 1

Figure 2

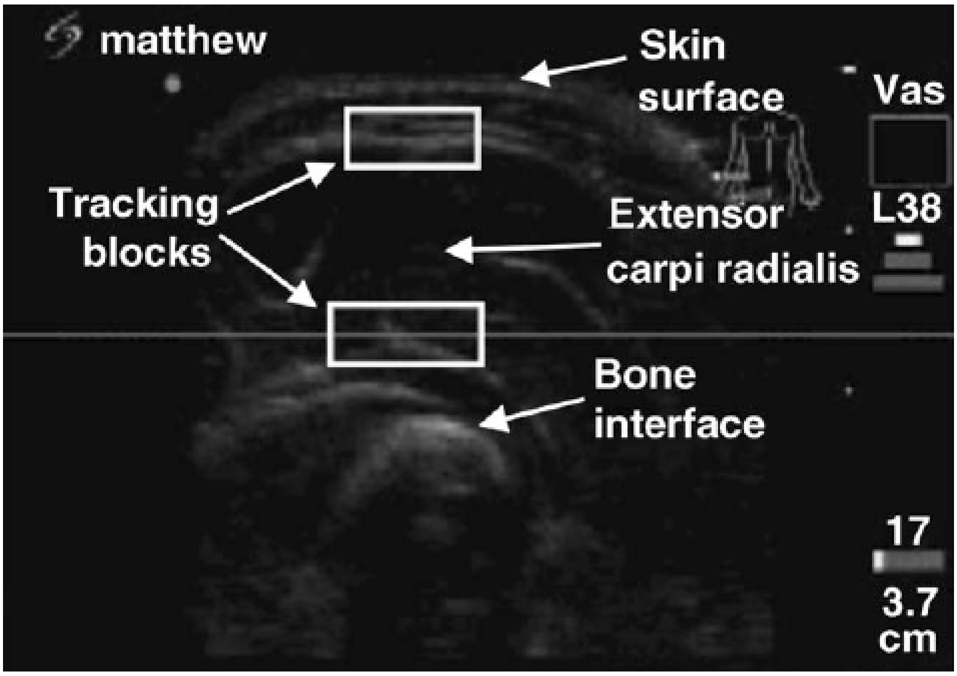

Figure 3

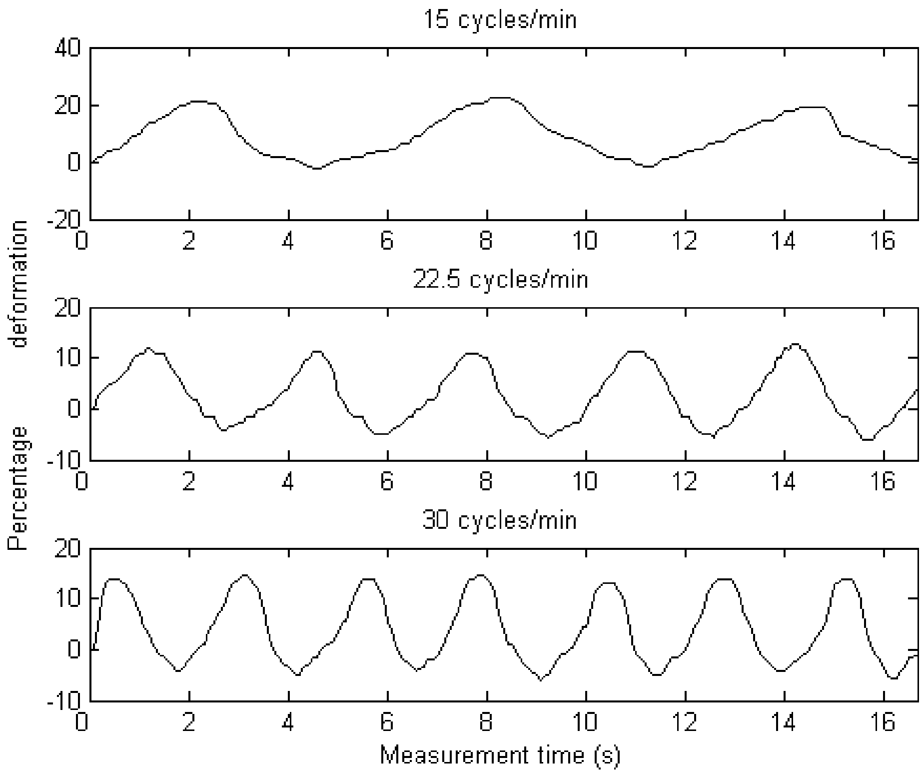

Figure 4

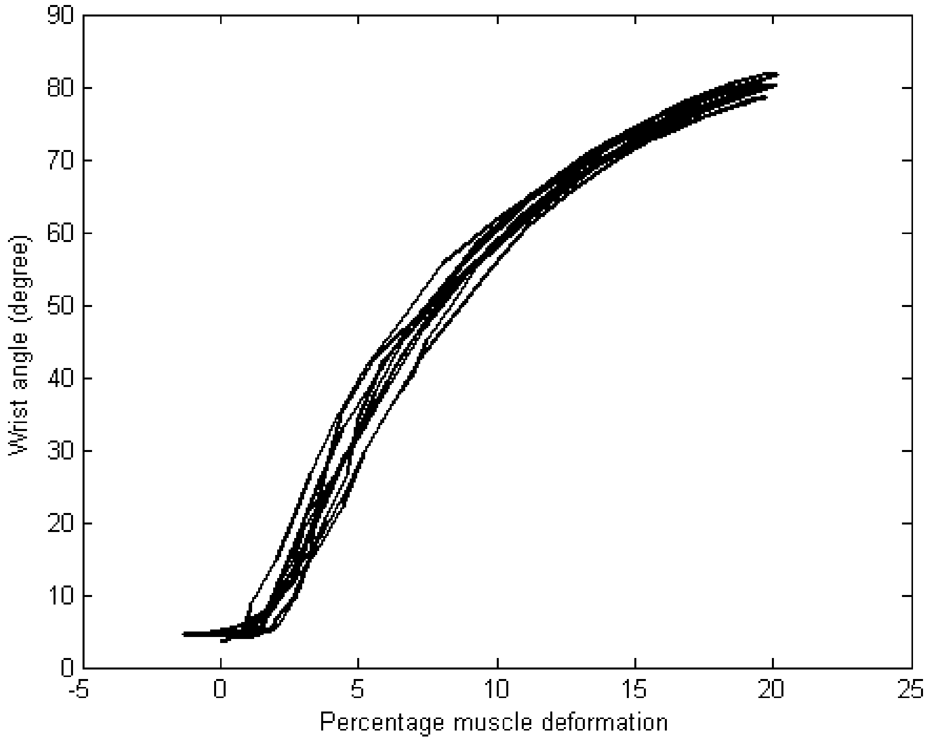

Figure 5

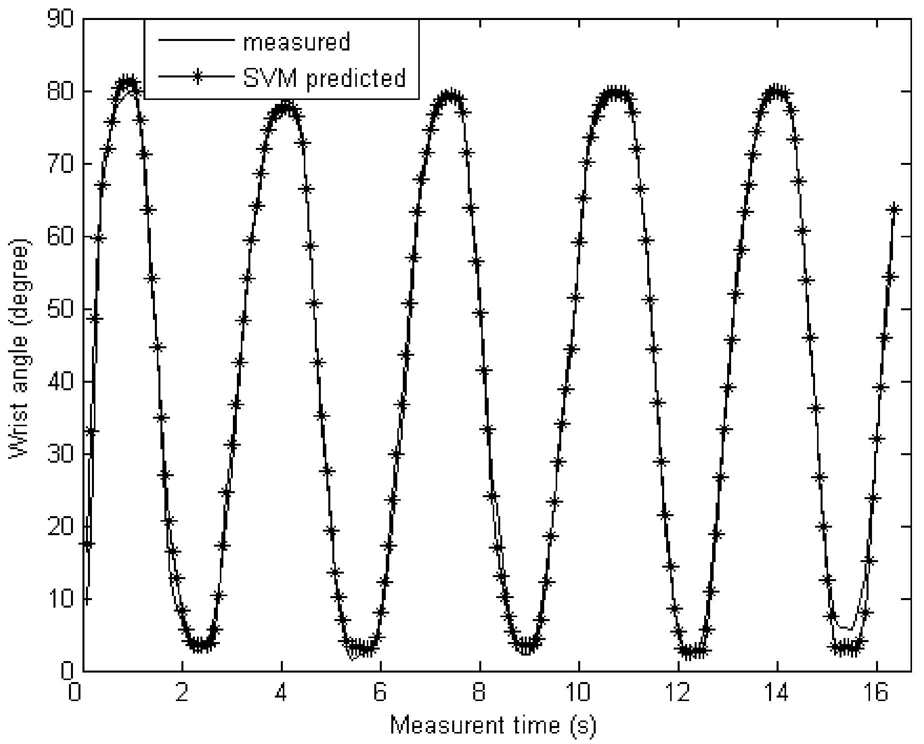

Figure 6

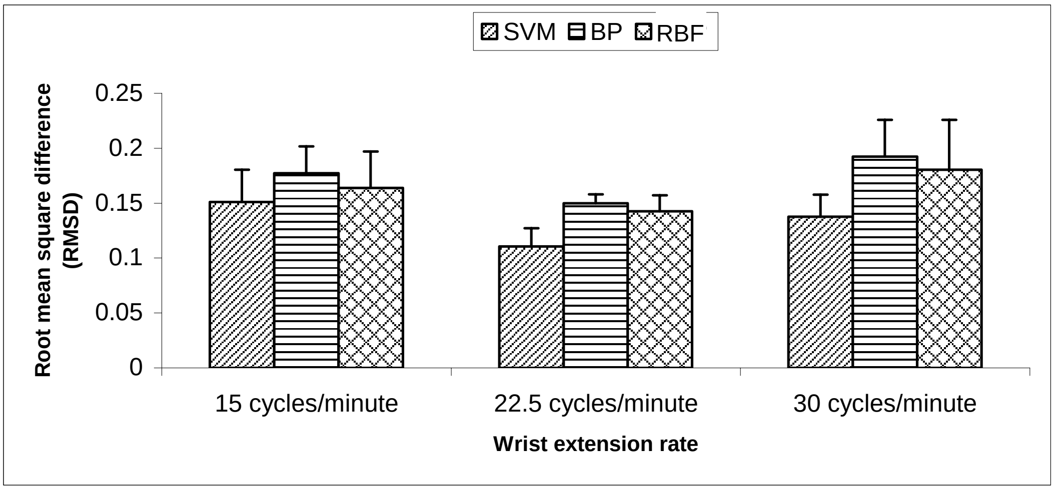

Figure 7

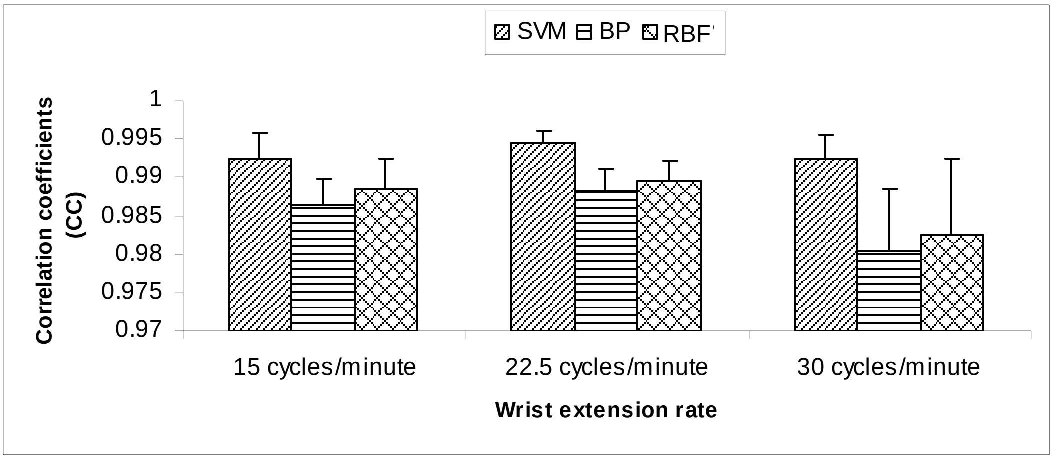

Figure 8

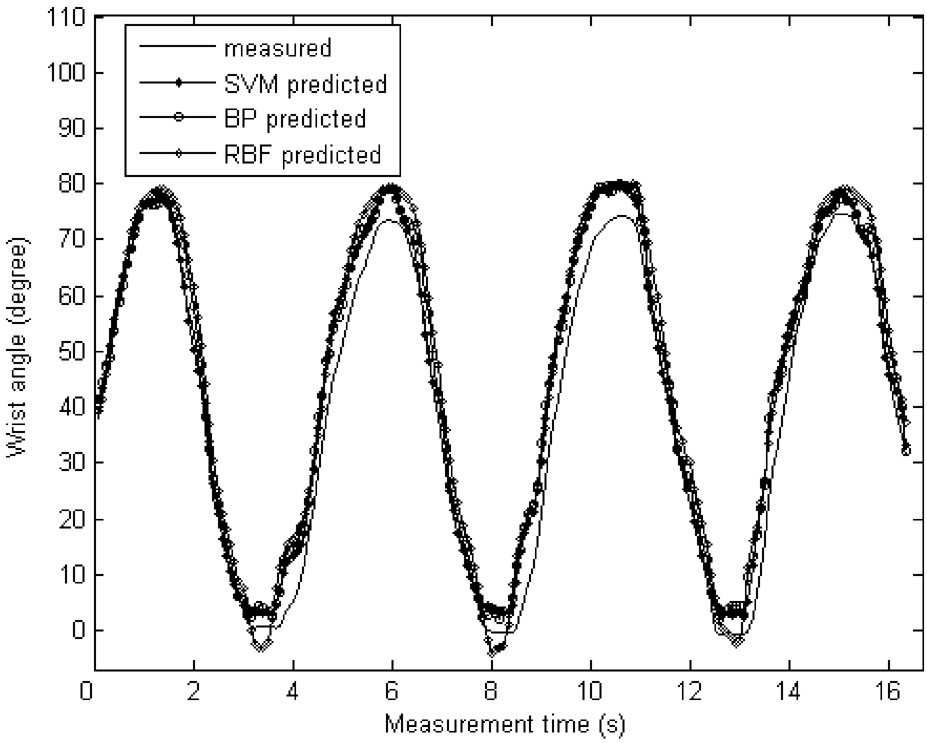

Figure 9

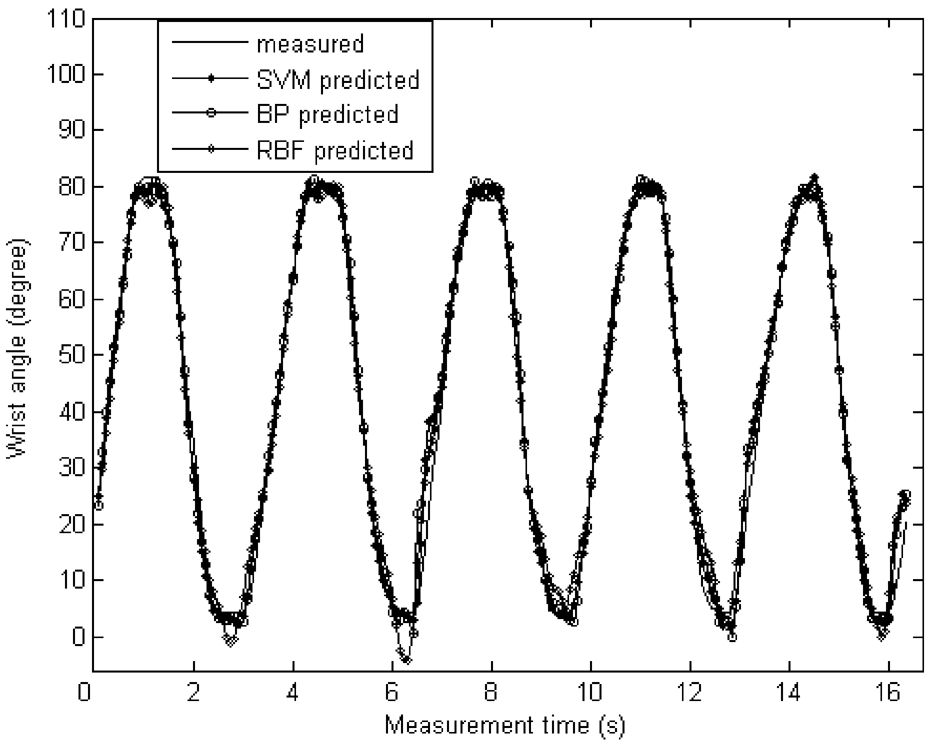

Figure 10

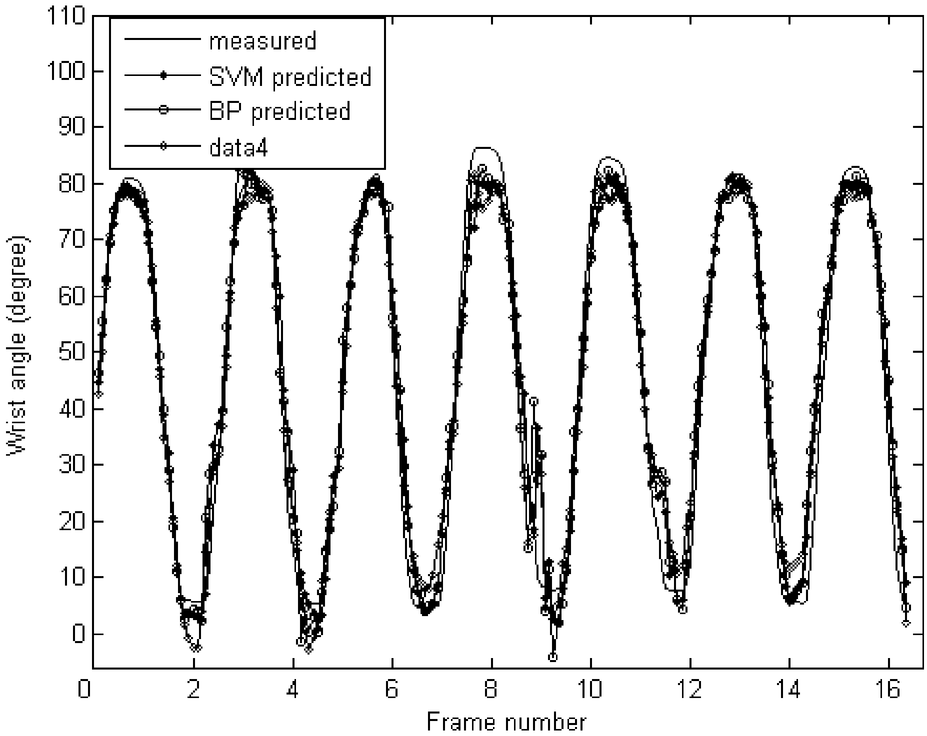
measured
SVM predicted
BP predicted
data4
Wrist angle (degree)
Frame number
110
100
90
80
70
60
50
40
30
20
10
0
0
2
4
6
8
10
12
14
16

Figure 11

Table captions

Table 1. The optimal LS-SVM hyperparameters for different subjects

Table 2. The results of one-way ANOVA for the prediction RMSD among the LS-SVM, BP and RBF methods

Table 3. The results of one-way ANOVA for the prediction CC among the LS-SVM, BP and RBF methods

Table1

subject	γ	δ^2
A	100	6
B	50	6
C	2000	2
D	2000	5
E	2500	5

Table 2

Prediction method	*p* value
LS-SVM versus BP network	0.0006
LS-SVM versus RBF network	0.0165
BP network versus RBF network	0.3612

Table 3

Prediction method	*p* value
LS-SVM versus BP network	0.0001
LS-SVM versus RBF network	0.0022
BP network versus RBF network	0.4627